Applied Catalysis B: Environmental 241 (2019) 570–577

Contents lists available at ScienceDirect

Applied Catalysis B: Environmental

journal homepage: www.elsevier.com/locate/apcatb

Sonocatalytic oxidation of EDTA in aqueous solutions over noble metal-free Co_3O_4/TiO_2 catalyst

Laureanne Parizot[a,b], Tony Chave[b], Maria-Elena Galvez[a], Hugo Dutilleul[a], Patrick Da Costa[a,*], Sergey I. Nikitenko[b,*]

[a] Jean Le Rond D'Alembert Institute, UPMC Sorbonne Universités, UPMC UNIV. Paris 6, CNRS UMR 7190, 2 place de la gare de ceinture, 78210 Saint Cyr L'Ecole, France
[b] Institut de Chimie Séparative de Marcoule (ICSM), UMR 5257, Univ. Montpellier- CEA-CNRS-ENSCM, Site de Marcoule, BP 17171, 30207 Bagnols sur Cèze Cedex, France

ARTICLE INFO

Keywords:
Sonochemistry
Ultrasound
Advanced oxidation processes
EDTA
Heterogeneous catalysis

ABSTRACT

The sonocatalytic degradation of EDTA in aqueous solution was studied under ultrasound irradiation (345 kHz, 73 W, acoustic power 0.20 W·mL^{-1}, Ar and Ar/O_2 saturating gases, T = 20–50 °C) in the presence of Co_3O_4/TiO_2 and Pt/TiO_2 nanocatalysts. About 90% of EDTA (C_0 = 5 10^{-3} M) was oxidized during ultrasonic treatment at 40 °C in the presence of the Co_3O_4/TiO_2 catalyst and Ar/O_2 gas mixture. By contrast, Pt/TiO_2 catalyst exhibited much lower sonocatalytic activity in this system. Suggested mechanism of EDTA oxidation in the presence of Co_3O_4/TiO_2 catalyst involved the generation of oxidizing radicals by acoustic cavitation and Co(II)-Co(III) redox process. Quite low apparent activation energy of the sonocatalytic process (E_a = 19 kJ mol^{-1}) was attributed to diffusion of reagents in the vicinity of the active sites of catalyst. Sonocatalytic degradation of EDTA is accompanied by formation of iminodiacetic acid, formic acid, oxalic acid, glycolic acid and acetic acid as intermediate products in an agreement with radical-driven mechanism.

1. Introduction

Ethylenediaminetetraacetic acid (EDTA) is widely used in food, cosmetic and pharmaceutical industries [1]. While EDTA is nontoxic itself, it is a metal-mobilizing pollutant that requires its removal from wastewater. In nuclear industry, EDTA is an obvious decontaminating agent due to its ability to form strong chelating complexes with a large number of radionuclides [2]. However, the formation of such complexes may impede further radionuclide removal from the liquid waste, *i.e.* through chemical precipitation or ion exchange [3]. Therefore, EDTA must be decomposed or at least defunctionalized prior to radionuclide specific treatments, whereas the methods of its decomposition should use minimal amounts of reagents, in order to minimize the volume of final waste. Advanced Oxidation Processes (AOP), based on the generation of highly reactive radical species, can potentially enable the effective oxidation of chelating agents in waste solutions [4]. Indeed, different AOPs have been lately considered for EDTA oxidation, such as catalytic Fenton-like processes [5,6], ozonolysis [7], hydrothermal oxidation [8], photolysis [9] and photocatalysis [10]. All of these techniques have some limitations, for instance, large amount of catalyst and H_2O_2 are required for Fenton processes. In the same way, ozone is not an eco-friendly and healthy product and the others treatments need high energy input. For all these reasons, researches have to be carried out to find more ecological and cost effective approaches for the treatment of wastewaters.

Among the different AOPs, sonochemistry stands as a promising technology that can provide an answer to this EDTA degradation issue. Indeed, this technique enables the in situ production of radical species. The chemical effects of power ultrasound come from acoustic cavitation, which is a set of consequent events: nucleation, growth and violent collapse of microbubbles in liquids submitted to ultrasonic vibrations. In aqueous solutions, cavitation causes splitting of water molecules leading to formation of $OH^{\cdot}$ radicals and H atoms, and to the products of their mutual recombination: H_2O_2 and H_2, respectively [11]. Recent spectroscopic studies of light emitted by collapsing bubbles, called sonoluminescence, revealed formation of nonequilibrium plasma inside the bubble [12]. Therefore, each cavitation bubble can be considered as microscopic plasma reactor producing highly reactive species in liquids at almost room bulk temperature. Indeed, the sonochemical degradation of EDTA in homogeneous aqueous solutions has been reported in the presence of oxygen [13] and hydrogen peroxide [14]. However, despite the extreme local conditions inside the cavitation bubbles, the overall reaction rate was found to be quite low. Sonochemical oxidation of EDTA can be significantly accelerated in the presence of zero-valent

* Corresponding authors.
E-mail addresses: patrick.da_costa@upmc.fr (P. Da Costa), serguei.nikitenko@cea.fr (S.I. Nikitenko).

https://doi.org/10.1016/j.apcatb.2018.09.001
Received 13 June 2018; Received in revised form 2 August 2018; Accepted 1 September 2018
Available online 15 September 2018
0926-3373/

iron particles *via* Fenton-like mechanism [15]. However, iron dissolution during this process would require additional purification stage after EDTA degradation.

It has been recently shown that power ultrasound accelerates the catalytic oxidation of carboxylic acids in the presence of powdered Pt/TiO_2 and Ar/O_2 gas mixtures [16]. The sonocatalytic effect was attributed to the strong dispersion of the Pt/TiO_2 catalyst together with the generation of chemically active species during water sonolysis. Though active, noble metals are quite expensive and, therefore, alternative catalytic systems need to be found. In the present paper we report, for the first time, quantitative sonochemical defunctionalization of EDTA in the presence of a noble metal-free catalyst Co_3O_4/TiO_2. Moreover, we found that Co_3O_4/TiO_2 exhibits much higher sonocatalytic activity than Pt/TiO_2 in studied reaction. Ultrasonic frequency and gas composition were chosen on the basis of previous researches [12,16].

2. Materials and methods

2.1. Reagents

Solids $Na_2H_2EDTA{\cdot}2H_2O$ (98%, Fluka AG), $Co(NO_3)_2{\cdot}6H_2O$ (98%, Alfa Aesar), TiO_2 anatase (99%, Sigma Aldrich, 95% anatase, 5% rutile), TiO_2 P25 (Aeroxide®, Evonik) and H_2PtCl_6 (999%, Strem) were used as received without further purification. All solutions were prepared with deionized water (Milli-Q 18.2 MΩ cm at 25 °C). Ar/O_2 gas mixture with 20 vol.% of O_2, Ar of 99.999% purity and O_2 99.999% purity were supplied by Air Liquide.

2.2. Synthesis of catalysts

Co_3O_4/TiO_2 catalysts with 6.4%wt., 3.3%wt. and 1.3%wt. of Co_3O_4 were prepared by excess solution impregnation using $Co(NO_3)_2{\cdot}6H_2O$ solution as cobalt precursor. The solution with suspended TiO_2 anatase powder was stirred one hour, and then dried at 65 °C for 30 min in a rotary evaporator. The resulting material was further dried in an oven at 80 °C for 20 min and subsequently calcinated at 550 °C for 4 h in order to ensure a maximal yield of crystallized Co_3O_4 [17].

Pt/TiO_2 catalyst was prepared by incipient wetness impregnation technique, using H_2PtCl_6 solution and P25 TiO_2 as the support for a Pt nominal content of 1%wt. After drying Pt(IV) was reduced with hydrazine hydrate solution, washed until the absence of chloride ions (control with Ag^+) and dried overnight under vacuum at room temperature. This technique enables a complete reduction of Pt(IV) at room temperature without modification of TiO_2 support [18].

2.3. Techniques of catalyst characterization

High-resolution transmission electron microscopy (TEM) measurements were carried out in a Jeol JEM 2200 FS device, equipped with a numeric camcorder. An ultrasonic bath was used to disperse the samples in deionized water. Then, one drop was deposited on carbon-coated copper grid and dried in atmospheric air prior to analysis. Powder XRD measurements were performed on the readily-prepared, fresh and used oxide catalysts in a Bruker D8 Advance Diffractometer, equipped with a Cu K_α (λ = 1.54056 Å) radiation source and a Lynx Eye detector. Powder XRD patterns were collected in the 10–90 2-theta degree range with a step size of 0.01° and a step time of 1 s. N_2-adsorption study at −196 °C was achieved with a BELSORB-Mini II device (BEL-Japan). Specific surface area was calculated with BET method. Temperature programmed reduction (H_2-TPR) was performed in a BELCAT-M apparatus from BEL Japan equipped with a thermal conductivity detector. In each experiment 60 mg of catalyst were degassed at 100 °C for 2 h and then heated to 900 °C at 7.5 °C min^{-1} heating rate in the presence of 5% vol. H_2/Ar gas mixture.

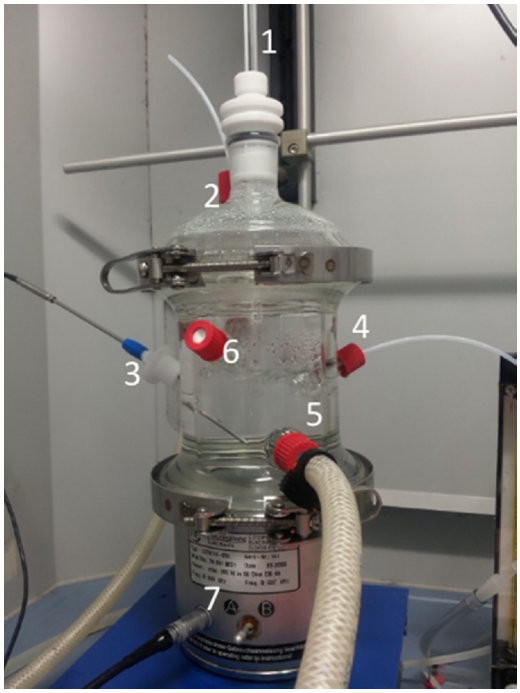

Fig. 1. Sonochemical reactor with (1) mechanical stirrer, (2) gas outlet, (3) thermocouple, (4) gas inlet, (5) water jacket, (6) sampling septum, (7) 345 kHz transducer.

2.4. EDTA degradation experiments

A home-made 400 mL glass reactor enabled the control of temperature and gas atmosphere was used in the experiments (Fig. 1). This reactor was fixed on the top of a 345 kHz transducer (ELAC Nautik, 25 cm^2), connected to a generator with a maximum electrical power of 125 W (T&C Power Conversion, Inc.). The electric load power was regulated at 73 W and the corresponding absorbed acoustic power was evaluated by thermal probe method at 0.20 W·mL^{-1}. The volume of sonicated solution was 200 mL, while additional mechanical stirring at 250 rpm was used in order to warranty a homogeneous suspension of catalyst particles [16]. The temperature during sonolysis was controlled between 20 and 50 °C with a Huber Unistat Tango thermo-cryostat and measured by a thermocouple immersed into ultrasound-irradiated solution. Ar/O_2 gas mixture was bubbled through solution for 20 min at 204 mL·min^{-1} flowrate before the experiment and kept during sonication. 400 mg of catalyst were dispersed in a minimal volume of water using ultrasonic bath prior to its injection to the EDTA solution. Sample aliquots were taken each hour to follow the evolution of EDTA, H_2O_2, intermediate degradation products and total organic carbon concentrations after their filtration using 0.2 µm PTFE membrane. No EDTA adsorption in sampling filters was observed, since the EDTA concentration measured in the first filtered aliquot extracted from the reactor during the silent catalytic experiment was identical to the nominal initial concentration of EDTA used in the experiment. All experiments were reproduced twice to verify the suitability of our uncertainties. Formed CO_2 was continuously monitored in the outlet gas using a Prima BT mass spectrometer (Thermo Scientific).

A Thermo Scientific Evolution 220 UV–vis spectrophotometer was used for the analysis either of EDTA, titrated using a $(Fe\text{-}TPTZ)^{2+}$ complex, where TPTZ stands for *Bis*(2,4,6- tripyridyl-*s*-triazine) [19], or of H_2O_2, titrated with $TiOSO_4$ [20]. The total carbon in solution was followed using a Shimadzu TOC-VCSH analyzer calibrated with potassium phthalate solution. Various intermediate degradation products of EDTA were detected by ion chromatography in a Dionex AS-AP device equipped with a capillary column AS11. The used eluent for the

measurement method was 10 mM KOH at 0.012 mL.min^{-1} and 40 °C. The identified species were glycolic, acetic, formic, oxalic and iminodiacetic acid in agreement with the literature [4].

The catalyst stability in reaction media, *i.e.* in the treated EDTA solution, was evaluated through the measurement of dissolved platinum and cobalt after catalytic and sonocatalytic experiments using a Spectro Arcos ICP-OES spectrometer. Prior to analysis, the solution samples were diluted in 0.3 M HNO_3, after catalyst separation with a 0.2 µm PTFE filter. ICP calibration curves were obtained using SCP Science standard solutions.

3. Results and discussion

3.1. Physico-chemical characterization of the Co_3O_4/TiO_2 and Pt/TiO_2 catalysts

All the catalysts prepared using cobalt salts were characterized upon their calcination, by means of both powder XRD and HRTEM techniques. In contrast, only HRTEM analysis was performed on the Pt/TiO_2 catalyst. The powder XRD patterns acquired for the Co-containing catalysts (JCPDS file no. 00-042-1467) confirmed the presence of cobalt oxide Co_3O_4 as the principal Co-phase, as well as of anatase, together with traces of rutile TiO_2 (Fig. S1 of the Supplementary data). The presence of these two TiO_2 phases is typical for commercial anatase product. In the case of 1.3%wt. Co_3O_4/TiO_2, the cobalt oxide phase was not detected in the diffractograms, most probably due to the low cobalt concentration in this catalyst.

The HRTEM/EDX images shown in Figs. 2 and 3 for 1.3%wt. and 6.4%wt. Co_3O_4/TiO_2 respectively and in Fig. S2 (Supplementary data) for 3.3%wt. Co_3O_4/TiO_2 evidence presence of cobalt oxide nanoparticles dispersed on the surface of TiO_2 support. The average size of Co_3O_4 nanoparticles calculated from HRTEM for each catalyst is shown in Table 1. Cobalt oxide nanoparticles around 10–15 nm are present in the 1.3%wt. Co_3O_4/TiO_2 catalyst. Higher Co-loading results in an increase of the average Co_3O_4 particle size, *i.e.* in the 3.3%wt. Co_3O_4/TiO_2 and 6.4%wt. Co_3O_4/TiO_2 catalysts the size of the Co_3O_4 particles reaches 15–20 nm. Also certain cobalt oxide agglomeration can be observed at HRTEM images at high Co-loading. Whereas, crystallite size calculated by Scherrer equation (Table 1) were found to be equal to 39.7 ± 7.5 nm for 3.3%wt. Co_3O_4/TiO_2 and 37.5 nm for 6.4%wt. Co_3O_4/TiO_2. These values are consistent with HRTEM measurements taking into account quite broad particle size distribution and uncertainties of both techniques. No XRD information could be obtained for the 1.3%wt. Co_3O_4 sample because of low cobalt concentration. The specific surface area (Table 1) was measured quite low compared to TiO_2 anatase specific surface area (45–55 m^2 g^{-1}) used in this work as well as other studies with TiO_2 support [21]. This could be attributed to the calcination at 550 °C which favorites aggregation of cobalt oxide and titanium oxide particles [22]. The HRTEM micrographs acquired for the Pt/TiO_2 catalyst are shown in Fig. 4 and reveal well dispersed 1–3 nm Pt nanoparticles on the TiO_2 support as it was already reported in the literature [16].

Fig. 5 shows the H_2-TPR profiles acquired for the different Co-containing catalysts. Table 2 summarizes the amounts of H_2 consumed during TPR experiments for each catalyst. As expected, increasing Co-loading leads to higher H_2-consumption during TPR, but this correlation is not directly proportional. TPR analysis reveals two reduction peaks common for all studied samples centered at 350 °C and 480–500 °C. According to the literature, the reduction of Co_3O_4 species on a TiO_2 surface is a 2-step process involving the consecutive reduction of Co(III) to Co(II) and Co(II) to metallic Co [21,23,24]. Therefore, a first peak at about 350 °C is expected to occur due to the reduction of Co_3O_4 to CoO, followed by a second peak at 450–500 °C attributed to the reduction of CoO to metallic Co. Surprisingly, an intermediate reduction peak appeared at 500 °C–520 °C for the samples with higher Co_3O_4 content. As previously commented, HRTEM pointed out some agglomeration of the Co-phase with increasing of Co-loading. The co-existence of Co_3O_4 particles of different size may account for the splitting of the low temperature H_2 consumption peak, *i.e.* larger Co_3O_4 particles will be reduced to CoO at higher temperatures [25]. The slight increase of the CoO reduction temperature from 500 °C to 520 °C with increasing of Co_3O_4 concentration from 3.3% to 6.4% (Fig. 5) can be attributed to the similar phenomenon. In the case of 2-step process, the area of the second peak should be three time more important than of the first one. However, in our study no direct relation could be found between each peak area. Then maybe, interaction with the support affects Co(III) and Co(II) reduction [21]. Another assumption could be the formation of intermediate nonstoichiometric cobalt oxides CoO_x during H_2-TPR reduction [26].

3.2. Catalytic activity in EDTA sonochemical oxidation

3.2.1. Non-catalytic EDTA sonochemical oxidation

In a first instance, the sonochemical oxidation of EDTA was studied in homogeneous aqueous solutions, *i.e.* in the absence of any catalyst. Thus, these results highlight the temperature and gas atmosphere influence the EDTA degradation rate and would allow further assess the benefit to add catalyst in the system. Kinetic curves shown in Fig. 6 point out overall zero-order reaction. The observed reaction rate of EDTA degradation slightly increased in the presence of oxygen, seeming

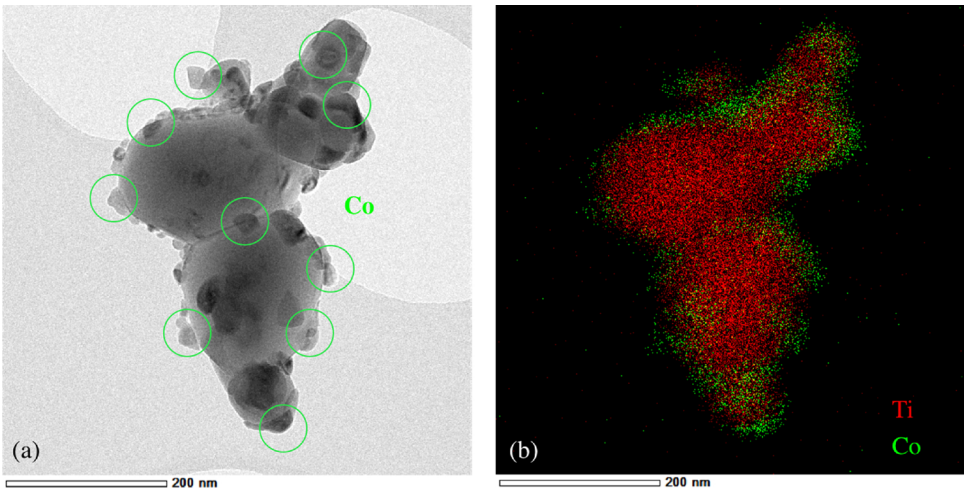

Fig. 2. TEM picture (a) and EDX map (b) for the 6.4% wt. Co_3O_4/TiO_2 catalyst.

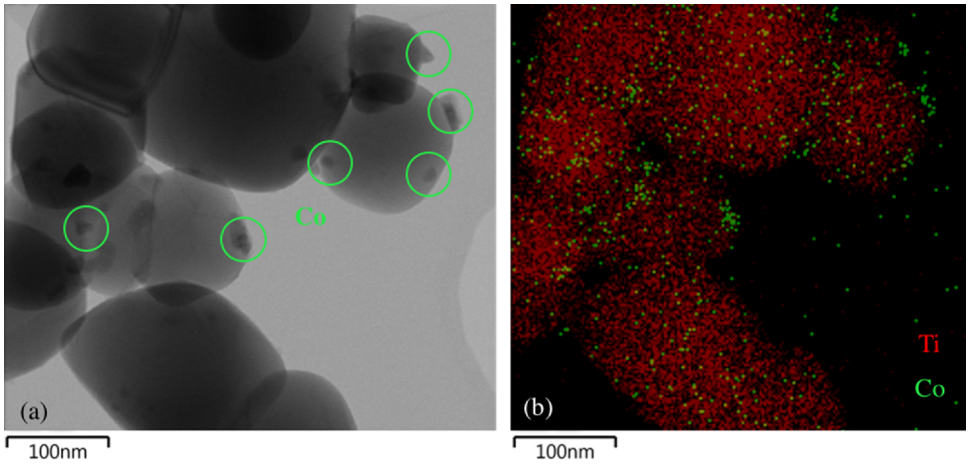

Fig. 3. TEM picture (a) and EDX map (b) for the 1.3% wt. Co_3O_4/TiO_2 catalyst.

Table 1
Co_3O_4 mean particle size obtained from HRTEM pictures and calculated from XRD patterns at 2-Thêta = 65.2° of Co_3O_4 using Scherrer equation, and specific surface area calculated by BET analysis. Particle size obtained by TEM was average from at least 20 parallel measurements.

	1.3%wt. Co_3O_4/TiO_2	3.3%wt. Co_3O_4/TiO_2	6.4%wt. Co_3O_4/TiO_2
TEM measurement	13.5 ± 3.6 nm	18.0 ± 5.2 nm	19.5 ± 3.8 nm
XRD measurement	–	39.7 ± 7.5 nm	37.5 ± 7.5 nm
Specific surface area	7.7 ± 1.5 $m^2 \cdot g^{-1}$	7.9 ± 1.5 $m^2 \cdot g^{-1}$	7.2 ± 1.5 $m^2 \cdot g^{-1}$

almost independent of the solution temperature in the range of 20–40 °C. In general, whatever the experimental conditions used, EDTA oxidation is quite slow in the absence of catalyst, as has been previously reported elsewhere [13].

Indeed, the slowest formation rate of H_2O_2 in the presence of EDTA than in water (Fig. 6b) suggests that the initial stage of EDTA sonochemical oxidation involves reactions with $OH^\cdot$ and $HO_2^\cdot$ radicals formed *via* water molecule splitting inside the cavitation bubbles:

$$H_2O \overset{)))}{\rightarrow} H^\cdot + OH^\cdot \quad (1)$$

$$2\ OH^\cdot \rightarrow H_2O_2 \quad (2)$$

$$H^\cdot + O_2 \rightarrow HO_2^\cdot \quad (3)$$

$$2\ HO_2^\cdot \rightarrow H_2O_2 \quad (4)$$

$$OH^\cdot + EDTA \rightarrow \text{Oxidation Products} \quad (5)$$

$$HO_2^\cdot + EDTA \rightarrow \text{Oxidation Products} \quad (6)$$

Actually, the Reactions (5) and (6) are competing with the reactions leading to H_2O_2 formation shown in the Eqs. (2) and (4). The plots in

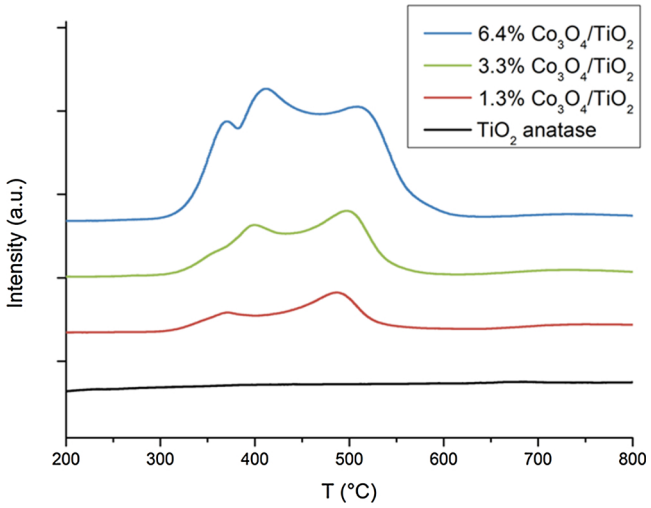

Fig. 5. H_2-TPR profiles acquired for the 1.3% wt. Co_3O_4/TiO_2, 3.3% wt. Co_3O_4/TiO_2 and 6.4% wt. Co_3O_4/TiO_2 catalysts.

Table 2
Hydrogen consumption during H_2-TPR runs performed on the Co-containing catalysts.

Co_3O_4/TiO_2 Catalyst	1.3%wt.	3.3%wt.	6.4%wt.
H_2 (μmol/g_{cat})	16.1	28.2	64.5

Fig. 6b show the H_2O_2 formation during water sonolysis and in presence of EDTA. The difference between these plots evidences that only about 40% of oxidizing radicals reacts with EDTA and intermediate

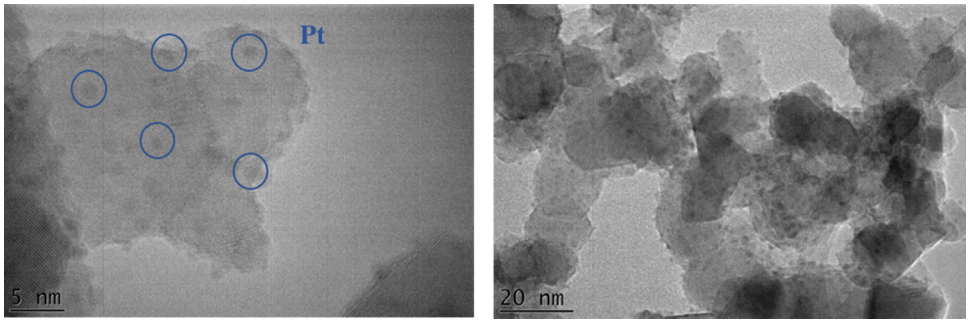

Fig. 4. HRTEM images of the 1% wt. Pt/TiO_2 catalyst.

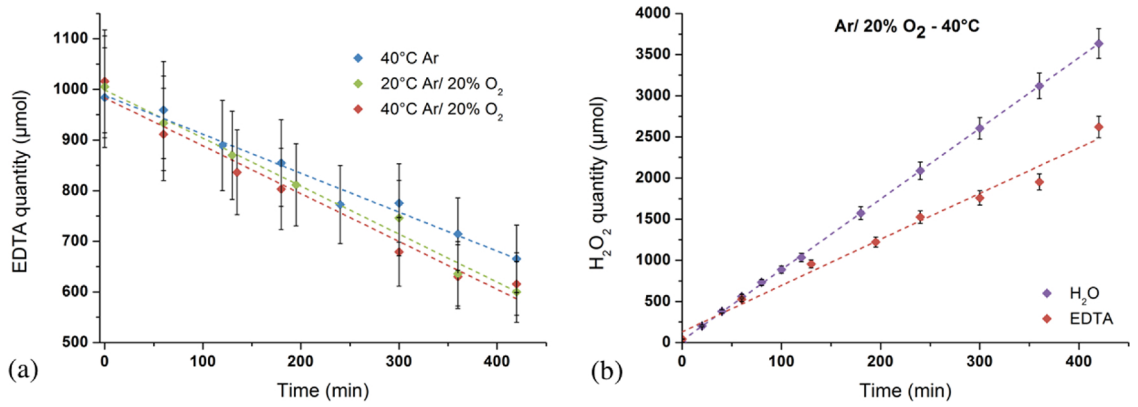

Fig. 6. (a) Evolution of EDTA amounts during sonolysis of homogeneous aqueous solutions as a function of temperature and various Ar/O_2 gas mixture composition. (b) Kinetic curves of H_2O_2 formation at 40 °C and Ar/20% O_2 gas atmosphere. The other conditions studied at 20 °C under Ar/20% O_2 gas mixture and at 40 °C under argon atmosphere are in Supplementary Data (Fig S3). V = 200 mL, $[EDTA]_0 = 5\ 10^{-3}$ M, under 345 kHz ultrasound (P_{ac} = 0.20 W mL^{-1}).

products, while the remaining recombine into H_2O_2. The H_2O_2 evolution under argon atmosphere at 40 °C and under Ar/20%O_2 atmosphere at 20 °C is represented in Fig. S3 of the Supplementary data. Similar H_2O_2 evolution plot profile at 20 °C and 40 °C confirms the temperature independence on the H_2O_2 production yield and the EDTA degradation yield in homogeneous solutions.

3.2.2. EDTA sonocatalytic oxidation

The sonochemical oxidation of EDTA is largely enhanced in the presence of Co_3O_4/TiO_2 catalyst. Fig. 7a shows that under the studied experimental conditions about 90% of EDTA can be oxidized upon 7 h ultrasonic treatment. Similar to homogeneous solutions, sonocatalytic reaction exhibits zero-order kinetics on EDTA. By contrast, the presence of Pt/TiO_2 enhances EDTA degradation of only 10% compared to sonochemical process without catalyst (Figs. 6a and 7b). This is a surprising result since noble metal-based catalysts usually show high catalytic performance in AOPs [16].

It is interesting to note that in the presence of pristine TiO_2 the reaction rate is very similar to that measured in homogeneous solutions, *i.e.* in absence of any solid material. This indicates that the active sites of the sonocatalytic reaction are situated on the surface of Co_3O_4 or Pt and not on TiO_2 support. However, both Co_3O_4/TiO_2 and Pt/TiO_2 were found to be completely inactive under silent conditions, *i.e.* under mechanical stirring without ultrasound. In the light of these results, the following mechanism of EDTA sonocatalytic degradation with the Co_3O_4/TiO_2 catalyst can be suggested: i) in a first step EDTA molecules are adsorbed on the surface of the Co_3O_4 sites, ii) Co(II) of Co_3O_4 mixed oxide is then oxidized to Co(III) by highly reactive radicals produced by

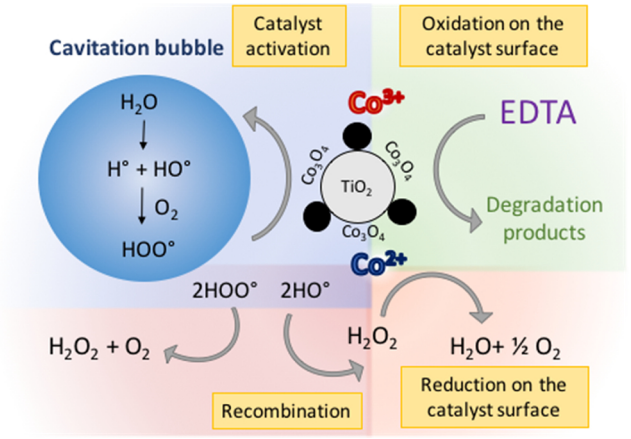

Fig. 8. Mechanism of EDTA sonocatalytic degradation in the presence of Co_3O_4/TiO_2 catalyst.

the cavitation bubbles, and iii) EDTA is finally oxidized by Co(III), being consequently reduced to Co(II). The proposed reaction mechanism depicted in Fig. 8 is confirmed by recently published data about strong interaction of EDTA molecules with Co_3O_4 surface [27]. The observed low catalytic performance of Pt/TiO_2 catalyst in studied process can be explained by the difference in the reaction mechanism which involves adsorption of O_2 molecules at Pt surface in a first step instead of EDTA molecule in the case of Co_3O_4/TiO_2 catalyst [16]. Therefore, the initial stage of EDTA sonocatalytic oxidation with Pt/

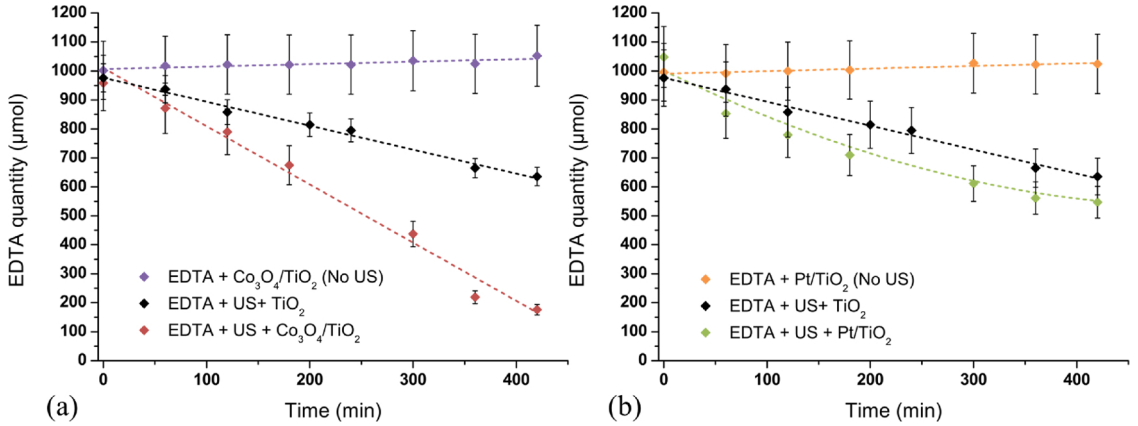

Fig. 7. Kinetic curves of EDTA sonocatalytic oxidation with 6.4%wt. Co_3O_4/TiO_2 (a) and 1% wt. Pt/TiO_2 (b). 345 kHz ultrasound or silent conditions (P_{ac} = 0.20 W mL^{-1}, T = 40 °C, Ar/20%O_2, catalyst concentration – 2 g L^{-1}).

TiO_2 catalyst would be limited by the reactions with radicals in homogeneous solution or cavitation bubble/solution interface rather than by redox process on Pt/TiO_2 surface.

For better understanding of the reaction mechanism, the influence of temperature on the sonocatalytic oxidation of EDTA was evaluated in the range of 20–50 °C. The derived Arrhenius linear plot is shown in Fig. S4 of the Supplementary data. The relatively low apparent activation energy calculated from these data ($E_a = 19 \pm 2\,kJ{\cdot}mol^{-1}$) suggests that the thermal effect is governed by reagent diffusion rather than by the splitting of EDTA chemical bonds, since the influence of the temperature on the intrinsic chemical reaction rate is expected to be much stronger [8]. Indeed, this conclusion is in line with the proposed radical-induced mechanism of EDTA sonocatalytic oxidation.

In order to elucidate the role of H_2O_2 in the reaction mechanism, the experiment of EDTA degradation was performed at 40 °C under mechanical stirring and $Ar/20\%O_2$ atmosphere without ultrasound in the presence of Co_3O_4/TiO_2 catalyst and under progressive addition of H_2O_2. No oxidation of EDTA was detected in this experiment indicating that H_2O_2 itself is not involved in the reaction mechanism. In contrast, quite rapid decomposition of H_2O_2 was observed with a rate of $2.4\,\mu mol\,min^{-1}$ in the presence of Co_3O_4/TiO_2 (Figs. 9 and S5 of the Supplementary data) in agreement with recently published results [28,29].

Table 3 summarizes the kinetics of EDTA degradation as a function of Co_3O_4 content. The normalized EDTA oxidation rate clearly increases with decreasing of cobalt oxide loading. This effect can be most probably attributed to the decrease of Co_3O_4 particle size with decreasing of Co_3O_4 content. According to literature, the enhanced catalytic activity of small Co_3O_4 nanoparticles is related to their higher surface density of Co(III) moieties [30,31]. It is noteworthy that Co(III) is known to form very strong complexes with EDTA [8], which subsequently leads to more efficient sonocatalytic oxidation.

Finally, the influence of oxygen concentration in Ar/O_2 gas mixture was investigated under the same reaction conditions ($2\,g\,L^{-1}$ of 6.4% wt. Co_3O_4/TiO_2, 40 °C, 200 mL, 5 mM EDTA, 345 kHz, $P_{ac} = 0.20\,W{\cdot}mL^{-1}$). Pure argon, $Ar/20\%O_2$ and $Ar/40\%O_2$ gas mixtures were used. The results are shown in Fig. S6 of the Supplementary data. Without oxygen in the system, EDTA degradation rate is very similar to the one observed under ultrasonic irradiation without catalyst. In addition, no significant differences were observed between 20% and 40% of oxygen in the gas mixture. One can conclude that oxygen is essential to provide maximal yield of $OH^{\cdot}$ and $HO_2^{\cdot}$ radicals *via* H atom scavenging without being a limiting species in this system.

3.2.3. Analysis of intermediate products

The plots shown in Fig. 10 evidence less effective TOC removal than EDTA degradation (Fig. 6a) which implies the formation of intermediate products. TOC data are supported by CO_2 mass spectrometric analysis in the outlet gas. For instance, in the experiment with Co_3O_4/TiO_2 catalyst 1.98 mmoL of CO_2 were measured corresponding to 2 mmoL TOC abatement (Fig. 10). Indeed, ion chromatography analysis allowed to identify the presence of iminodiacetic acid, formic acid, oxalic acid, glycolic acid and acetic acid in the solutions treated with ultrasound. Chemical structure of these products and typical chromatograms are shown in Figs. S7 and S8 of the Supplementary data respectively. The concentrations of these products measured after 7 h of sonolysis are summarized in Fig. 11. The fragments of EDTA degradation observed in our experiments are very similar to those reported for EDTA γ-radiolysis in oxygenated solutions [32]. Radiolytic degradation of EDTA occurs *via* the reactions with $OH^{\cdot}$ and $HO_2^{\cdot}$ radicals. Therefore, the similarity of the intermediate products for both processes would indicate the radical mechanism of EDTA sonocatalytic degradation. Iminodiacetic acid is formed at the earlier stage of EDTA oxidation. By contrast, formic acid is a product of deep EDTA degradation. Consequently, lower concentration of iminodiacetic acid and higher concentration of formic acid in solution treated with Co_3O_4/TiO_2 catalyst compared to sonicated homogeneous solution indicate more profound EDTA degradation in sonocatalytic process.

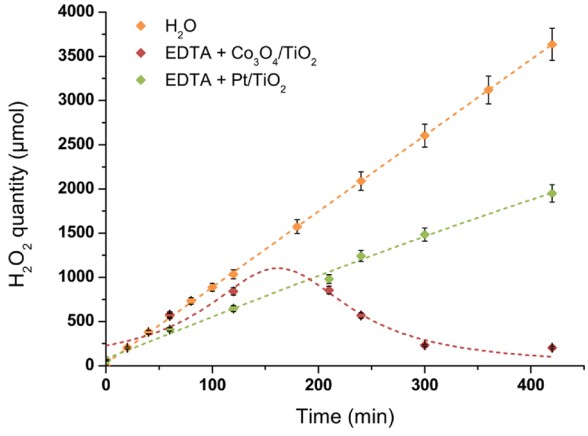

Fig. 9. Evolution of H_2O_2 quantity under 345 kHz ultrasound ($P_{ac} = 0.20\,W\,mL^{-1}$, T = 40 °C, $Ar/20\%O_2$).

Table 3
EDTA degradation rate (W, $mmol\,h^{-1}{\cdot}g_{Co}{}^{-1}$) normalized to cobalt mass in catalyst ($2\,g\,L^{-1}$). f = 345 kHz, $P_{ac} = 0.20\,W{\cdot}mL^{-1}$, T = 40 °C, $Ar/20\%O_2$. The error of W measurements was about 10%.

Co_3O_4/TiO_2 Catalyst	6.4%wt.	3.3%wt.	1.3%wt.
W ($mmol\,h^{-1}\,g_{Co}{}^{-1}$)	6.4	12.7	32.9

The ultrasonic irradiation in the presence of Pt/TiO_2 catalyst is less effective for TOC removal compared to Co_3O_4/TiO_2 catalyst (Fig. 10), which agrees with general lower catalytic activity of platinized catalyst for EDTA oxidation. On the other hand, the concentrations of iminodiacetic acid, formic acid and oxalic acid are clearly lower in the presence of Pt/TiO_2 particles than in homogeneous solutions (Fig. 11). Therefore, one can conclude that this catalyst improves the degradation of intermediates, which lead to somewhat better TOC abatement compared to homogeneous solution (Fig. 10). This is traced back to the difference in the reaction mechanisms with Co_3O_4/TiO_2 and Pt/TiO_2 catalysts. In the case of Pt/TiO_2, the principal mechanism related to the activation of O_2 molecules on Pt surface provides better efficiency for oxidation of small carboxylic acids [16] formed as intermediates during sonochemical degradation of EDTA.

Thorough chemical analysis allowed to establish a carbon balance in solution summarized in Fig. S8 of the Supplementary data. In sonocatalytic process with Co_3O_4/TiO_2, some unidentified species can reach 35% of initial carbon balance. On the other hand, the concentration of such products is negligible for the process in homogeneous solution which can be related to some difference in the reaction mechanism with and without catalyst.

3.2.4. Catalyst stability

The stability of both catalysts was assessed in the presence of 5 mM EDTA with mechanical stirring and Ar/O_2 atmosphere under ultrasonic irradiation and silent conditions during 7 h at 40 °C. ICP OES analysis showed that only 0.2% and 1.4% for Pt and Co respectively of an equivalent metal quantity were leached into the solution under ultrasound. Metal leaching under silent conditions was found to be equal to 0.2% and 2% for Pt and Co respectively. These results are within the ICP technique uncertainty and point out a good catalyst stability, and practically rules out the possibility of any secondary homogeneous oxidation reaction occurring within the liquid phase.

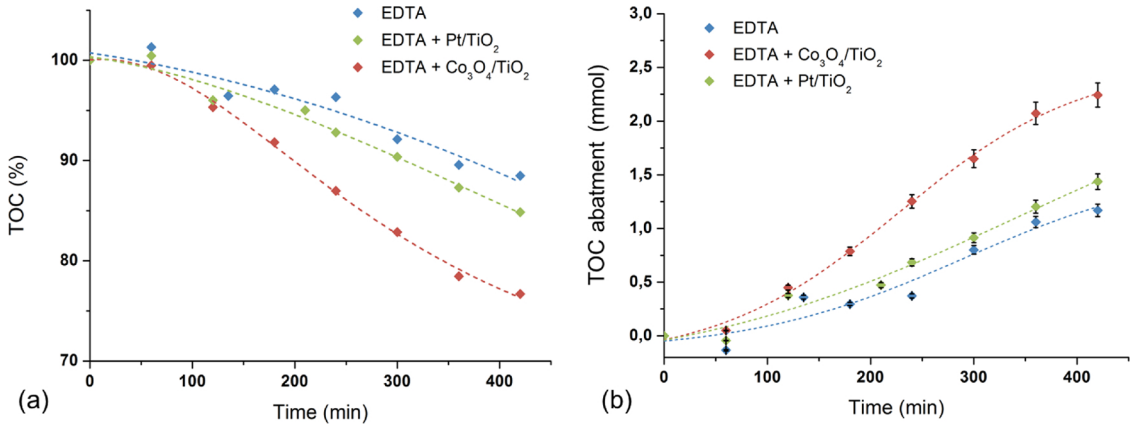

Fig. 10. Kinetics of TOC removal expressed in % (a) and mmol (b) during sonolysis of EDTA homogeneous solution and heterogeneous system with 6.4%wt. Co_3O_4/TiO_2 catalyst and 1%wt. Pt/TiO_2 (2 gL^{-1} of catalyst, 40 °C, 200 mL, 5 mM EDTA, f = 345 kHz, P_{ac} = 0.20 $W{\cdot}mL^{-1}$, 20%O_2/Ar). TOC measurement error was about 5%.

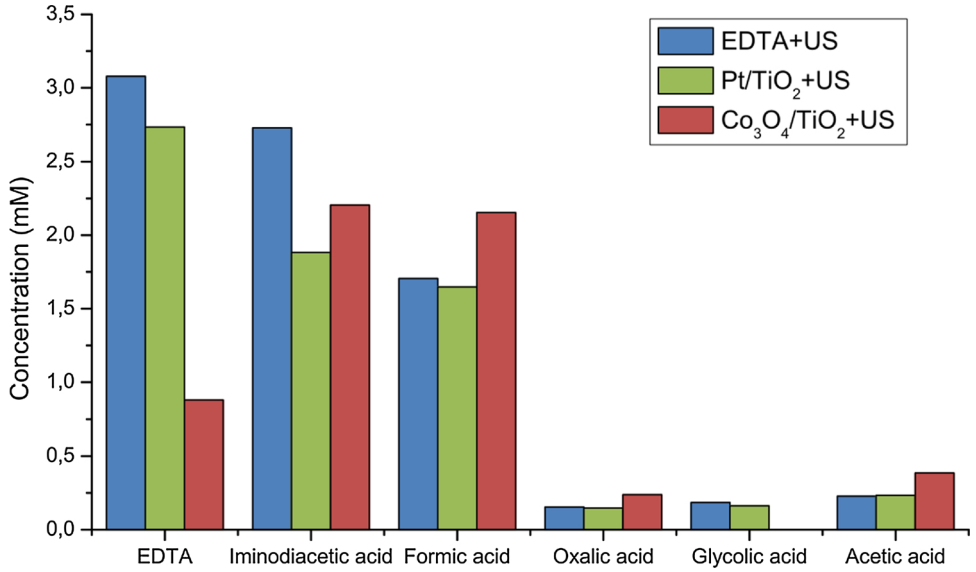

Fig. 11. Intermediate products of EDTA solutions (2 g L^{-1} of 6.4% wt. Co_3O_4/TiO_2 or 1% wt. Pt/TiO_2, 40 °C, 200 mL, 5 mM EDTA, f = 345 kHz, P_{ac} = 0.20 W mL^{-1}, 20%O_2/Ar). Concentration error was about 10%.

3.2.5. *Characterization of the spent catalysts*

The Co-containing catalysts where characterized by XRD, BET and H_2-TPR upon their exposure to ultrasound irradiation during the sonocatalytic experiments. XRD measurements of spent 6.4%wt. Co_3O_4/TiO_2 catalyst show the same patterns as initial catalyst. The crystallite size of Co_3O_4 and the specific surface area of spent Co_3O_4/TiO_2 catalyst were also found practically equal to that before the sonocatalytic treatment (37.8 ± 7.5 nm and 6.9 ± 1.5 $m^2\,g^{-1}$ respectively). So, this catalyst was apparently stable during 7 h of ultrasonic treatment.

The H_2-TPR profiles acquired for the fresh and spent 6.4%wt. Co_3O_4/TiO_2 catalysts are shown in Fig. 12. The profile obtained for the spent catalyst differs from that acquired for the fresh catalyst indicating a redistribution of the Co-active sites upon the sonocatalytic reaction. The main reduction peaks are still present, however, their intensity and appearance clearly change. In addition, lower H_2-consumption was obtained for the spent catalysts (25.5 µmol/$g_{catalysts}$) than for the fresh one (64.5 µmol/$g_{catalysts}$, Table 2), indicating the presence of already reduced Co-species upon the sonocatalytic reaction. This observation further confirms the sonocatalytic mechanism proposed in Fig. 8 involving Co(II)-Co(III) redox process in the reaction mechanism. Absence of Co(II) moieties in the DRX patterns of spent catalyst most likely is related to their low concentrations.

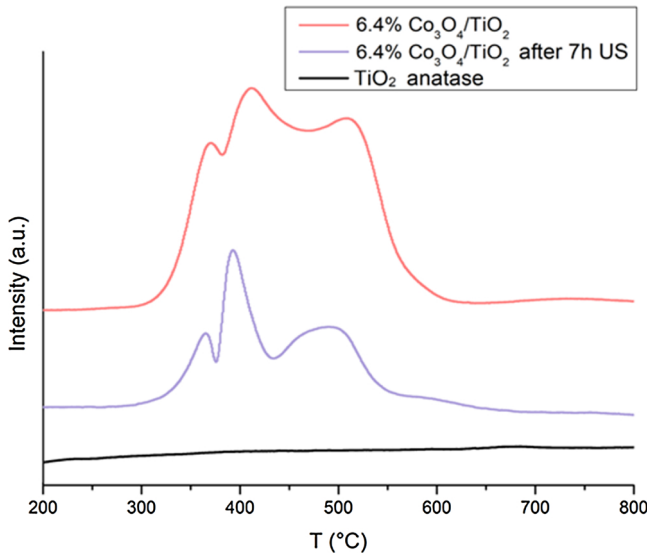

Fig. 12. H_2-TPR profiles acquired for the 6.4% wt. Co_3O_4/TiO_2 catalyst, before and after the sonocatalytic test.

4. Conclusions

The present study reveals advanced sonocatalytic activity of Co_3O_4/TiO_2 noble metal-free catalyst in the reaction of EDTA oxidation. Quantitative EDTA degradation can be reached using high-frequency 345 kHz ultrasound and Ar/O_2 gas atmosphere at near-room temperature. Surprisingly, the sonocatalytic activity of Co_3O_4/TiO_2 was found to be significantly higher than that of traditional Pt/TiO_2 catalyst. This striking phenomenon can be attributed to the stronger interaction of EDTA with Co_3O_4 compared to metallic platinum. It is interesting to note that both catalysts are inactive under silent conditions. We suggest that the mechanism of sonocatalytic process involves the adsorption of EDTA at the cobalt oxide sites, the production of oxidizing radicals during cavitation bubble collapse and redox reaction at Co_3O_4 surface intermediated by Co(II)-Co(III) electron transfer. Relatively low activation energy of the overall process equal to $E_a = 19\,kJ\,mol^{-1}$ pointed out that the thermal effect is related to reagent diffusion rather than to excitation of chemical bonds. Sonochemical and sonocatalytic degradation of EDTA is accompanied by formation of several acidic intermediates, such as iminodiacetic acid, formic acid, oxalic acid, glycolic acid, and acetic acid. Similar intermediates have been observed during radical degradation of EDTA induced by γ-irradiation. Despite low catalytic activity toward EDTA oxidation, Pt/TiO_2 catalyst improves sonochemical degradation of intermediate products compared to homogeneous solutions. To conclude, these results revealed a new possibility to decompose persistent organic pollutants, such as EDTA, with noble metal-free catalyst.

Acknowledgements

Work performed within the Investments for the future program of the French Government and operated by the French National Radioactive Waste Management Agency (ANDRA), Project CADET. Xavier Le Goff, Cyrielle Rey and Gaëlle Denion are acknowledged for HRTEM, ion chromatography analysis and participating in experiments.

Appendix A. Supplementary data

Supplementary material related to this article can be found, in the online version, at doi:https://doi.org/10.1016/j.apcatb.2018.09.001.

References

[1] J.R. Hart, Ethylenediaminetetraacetic Acid and Related Chelating Agents, in: Wiley-VCH Verlag GmbH & Co. KGaA (Ed.), Ullmanns Encycl. Ind. Chem. Wiley-VCH Verlag GmbH & Co. KGaA, Weinheim, Germany, 2000.
[2] J. Severa, J. Bár, Handbook of Radioactive Contamination and Decontamination, Elsevier, Amsterdam; New York, 1991.
[3] E.K. Papynov, M.S. Palamarchuk, V.Y. Mayorov, E.B. Modin, A.S. Portnyagin, T.A. Sokol'nitskaya, A.A. Belov, I.G. Tananaev, V.A. Avramenko, Sol–gel (template) synthesis of macroporous Mo-based catalysts for hydrothermal oxidation of radionuclide-organic complexes, Solid State Sci. 69 (2017) 31–37.
[4] M.E.T. Sillanpää, T. Agustiono Kurniawan, W. Lo, Degradation of chelating agents in aqueous solution using advanced oxidation process (AOP), Chemosphere 83 (2011) 1443–1460.
[5] K.A. Sashkina, A.V. Polukhin, V.S. Labko, A.B. Ayupov, A.I. Lysikov, E.V. Parkhomchuk, Fe-silicalites as heterogeneous Fenton-type catalysts for radiocobalt removal from EDTA chelates, Appl. Catal. B Environ. 185 (2016) 353–361.
[6] J.D. Englehardt, D.E. Meeroff, L. Echegoyen, Y. Deng, F.M. Raymo, T. Shibata, Oxidation of aqueous EDTA and associated organics and coprecipitation of inorganics by ambient iron-mediated aeration, Environ. Sci. Technol. 41 (2007) 270–276.
[7] E. Gilbert, S. Hoffmann-Glewe, Ozonation of ethylenediaminetetraacetic acid (EDTA) in aqueous solution, influence of pH value and metal ions, Water Res. 24 (1990) 39–44.
[8] V.A. Avramenko, A.V. Voit, E.E. Dmitrieva, V.G. Dobrzhanskii, V.S. Maiorov, V.I. Sergienko, S.I. Shmatko, Hydrothermal oxidation of Co-EDTA complexes, Dokl. Chem. 418 (2008) 19–21.
[9] A.F. Seliverstov, B.G. Ershov, Y.O. Lagunova, P.A. Morozov, A.S. Kamrukov, S.G. Shashkovskii, Oxidative degradation of EDTA in aqueous solutions under UV irradiation, Radiochemistry 50 (2008) 70–74.
[10] H. Seshadri, P.K. Sinha, Efficient decomposition of liquid waste containing EDTA by advanced oxidation nanotechnology, J. Radioanal. Nucl. Chem. 292 (2012) 829–835.
[11] T.J. Mason, J.P. Lorimer, Applied Sonochemistry: Uses of Power Ultrasound in Chemistry and Processing, Wiley-VCH Verlag GmbH & Co., KGaA, Weinheim, FRG, 2002.
[12] S.I. Nikitenko, R. Pflieger, Toward a new paradigm for sonochemistry: short review on nonequilibrium plasma observations by means of MBSL spectroscopy in aqueous solutions, Ultrason. Sonochem. 35 (2017) 623–630.
[13] J.A. Frim, J.F. Rathman, L.K. Weavers, Sonochemical destruction of free and metal-binding ethylenediaminetetraacetic acid, Water Res. 37 (2003) 3155–3163.
[14] S. Chitra, K. Paramasivan, P.K. Sinha, K.B. Lal, Ultrasonic treatment of liquid waste containing EDTA, J. Clean. Prod. 12 (2004) 429–435.
[15] T. Zhou, T.-T. Lim, Y. Li, X. Lu, F.-S. Wong, The role and fate of EDTA in ultrasound-enhanced zero-valent iron/air system, Chemosphere 78 (2010) 576–582.
[16] T. Chave, N.M. Navarro, P. Pochon, N. Perkas, A. Gedanken, S.I. Nikitenko, Sonocatalytic degradation of oxalic acid in the presence of oxygen and Pt/TiO_2, Catal. Today. 241 (2015) 55–62.
[17] M. Del Arco, V. Rives, Interactions with the support in Co/TiO_2 and Co_3O_4/TiO_2 systems, J. Mater. Sci. 21 (1986) 2938–2940.
[18] B. Beyribey, B. Corbacioğlu, Z. Altin, Synthesis of platinum particles from H_2PtCl_6 with hydrazine as reducing agent, Gazi Univ. J. Sci. 22 (2009) 351–357.
[19] B. Kratochvil, M. Clasby White, Spectrophotometric determination of microgram quantities of (ethylenedinitrilo)tetraacetic acid with bis(2/4,6-tripyridyl-s-triazine) iron(ll), Anal. Chem. 37 (1965) 111–113.
[20] D.W. O'Sullivan, M. Tyree, The kinetics of complex formation between Ti(IV) and hydrogen peroxide, Int. J. Chem. Kinet. 39 (2007) 457–461.
[21] J. Li, G. Lu, G. Wu, D. Mao, Y. Guo, Y. Wang, Y. Guo, Effect of TiO_2 crystal structure on the catalytic performance of Co_3O_4/TiO_2 catalyst for low-temperature CO oxidation, Catal. Sci. Technol. 4 (2014) 1268–1275.
[22] X. Chen, J.P. Cheng, Q.L. Shou, F. Liu, X.B. Zhang, Effect of calcination temperature on the porous structure of cobalt oxide micro-flowers, Cryst. Eng. Comm. 14 (2012) 1271–1276.
[23] B.M. Xaba, J.P.R. de Villiers, Sintering behavior of TiO_2 -supported model cobalt Fischer–Tropsch catalysts under H_2 reducing conditions and elevated temperature, Ind. Eng. Chem. Res. 55 (2016) 9397–9407.
[24] K. Takanabe, K. Nagaoka, K. Nariai, K. Aika, Titania-supported cobalt and nickel bimetallic catalysts for carbon dioxide reforming of methane, J. Catal. 232 (2005) 268–275.
[25] F. Huang, C. Chen, F. Wang, B. Wang, L. Zhang, S. Lu, K. Li, Effect of calcination temperature on the catalytic oxidation of formaldehyde over Co_3O_4-CeO_2 catalysts, Catal. Surv. Asia 21 (2017) 143–149.
[26] S. Capela, R. Catalão, P. Da Costa, G. Djéga-Mariadassou, F.R. Ribeiro, F. Ribeiro, C. Henriques, Metallic active species for de NO_x SCR by methane with Co and Pd/Co HFER catalysts, Stud. Surf. Sci. Catal. (2008) 1033–1038 Elsevier.
[27] H. Zhou, M. Kang, D. Wu, B. Lv, Synthesis and catalytic property of facet-controlled Co_3O_4 structures enclosed by (111) and (113) facets, Cryst. Eng. Comm. 18 (2016) 5456–5462.
[28] G.A. El-Shobaky, A.E.-M.M. Turky, Catalytic decomposition of H_2O_2 on Co_3O_4 doped with MgO and V_2O_5, Colloids Surf. Physicochem. Eng. Asp. 170 (2000) 161–172.
[29] J. Dong, L. Song, J.-J. Yin, W. He, Y. Wu, N. Gu, Y. Zhang, Co_3O_4 Nanoparticles with multi-enzyme activities and their application in immunohistochemical assay, ACS Appl. Mater. Interfaces 6 (2014) 1959–1970.
[30] V. Iablokov, R. Barbosa, G. Pollefeyt, I. Van Driessche, S. Chenakin, N. Kruse, Catalytic CO oxidation over well-defined cobalt oxide nanoparticles: size-reactivity correlation, ACS Catal. 5 (2015) 5714–5718.
[31] S. Sadasivan, R.M. Bellabarba, R.P. Tooze, Size dependent reduction-oxidation-reduction behaviour of cobalt oxide nanocrystals, Nanoscale 5 (2013) 11139.
[32] B. Höbel, C. von Sonntag, OH-radical induced degradation of ethylenediaminetetraacetic acid (EDTA) in aqueous solution: a pulse radiolysis study, J. Chem. Soc. Perkin Trans. 2 (1998) 509–514.